COLD SPRING HARBOR
Molecular Case Studies

RESEARCH ARTICLE

A common founding clone with *TP53* and *PTEN* mutations gives rise to a concurrent germ cell tumor and acute megakaryoblastic leukemia

Charles Lu,[1,5] Peter Riedell,[2,5] Christopher A. Miller,[1,3] Ian S. Hagemann,[4] Peter Westervelt,[2] Bradley A. Ozenberger,[1] Michelle O'Laughlin,[1] Vincent Magrini,[1] Ryan T. Demeter,[1] Eric J. Duncavage,[4] Malachi Griffith,[1] Obi L. Griffith,[1,2] and Lukas D. Wartman[1,2]

[1]McDonnell Genome Institute, Washington University School of Medicine, St. Louis, Missouri 63110, USA; [2]Division of Oncology, Department of Medicine, Washington University School of Medicine, St. Louis, Missouri 63110, USA; [3]Division of Genomics and Bioinformatics, Department of Medicine, Washington University School of Medicine, St. Louis, Missouri 63110, USA; [4]Department of Pathology and Immunology, Washington University School of Medicine, St. Louis, Missouri 63110, USA

Abstract We report the findings from a patient who presented with a concurrent mediastinal germ cell tumor (GCT) and acute myeloid leukemia (AML). Bone marrow pathology was consistent with a diagnosis of acute megakaryoblastic leukemia (AML M7), and biopsy of an anterior mediastinal mass was consistent with a nonseminomatous GCT. Prior studies have described associations between hematological malignancies, including AML M7 and nonseminomatous GCTs, and it was recently suggested that a common founding clone initiated both cancers. We performed enhanced exome sequencing on the GCT and the AML M7 from our patient to define the clonal relationship between the two cancers. We found that both samples contained somatic mutations in *PTEN* (C136R missense) and *TP53* (R213 frameshift). The mutations in *PTEN* and *TP53* were present at ~100% variant allele frequency (VAF) in both tumors. In addition, we detected and validated five other shared somatic mutations. The copy-number analysis of the AML exome data revealed an amplification of Chromosome 12p. We also identified a heterozygous germline variant in *FANCA* (S858R), which is known to be associated with Fanconi anemia but is of uncertain significance here. In summary, our data not only support a common founding clone for these cancers but also suggest that a specific set of distinct genomic alterations (in *PTEN* and *TP53*) underlies the rare association between GCT and AML. This association is likely linked to the treatment resistance and extremely poor outcome of these patients. We cannot resolve the clonal evolution of these tumors given limitations of our data.

[Supplemental material is available for this article.]

Corresponding author:
lwartman@dom.wustl.edu

Ontology terms: hematological neoplasm, neoplasm of the genitourinary tract

Published by Cold Spring Harbor Laboratory Press

doi: 10.1101/mcs.a000687

INTRODUCTION

Since first recognized in 1985, multiple studies have described the unique and rare association between hematological malignancies and germ cell tumors (GCTs) (DeMent et al.

[5]These authors contributed equally to this work.

1985; Nichols et al. 1985, 1990; Woodruff et al. 1995; Hartmann et al. 2000). Most commonly, these cases involve the megakaryocytic lineage of hematopoiesis, frequently resulting in acute megakaryoblastic leukemia (AML M7) and primary mediastinal nonseminomatous GCTs. Initially, the biologic relationship between these two entities was elusive, but the first definitive overview of the syndrome by Nichols et al. (1990) described the significance of an isochromosome 12p in the acute myeloid leukemia (AML) samples from these patients in that it "suggests that the hematologic neoplasm and the mediastinal germ-cell tumor arose from a common progenitor cell" (Hartmann et al. 2000). Isochromosome 12p is the most common chromosomal abnormality identified in GCTs but is exceedingly rare in AML that is not associated with a GCT (Gibas et al. 1986; Hartmann et al. 2000). A potential shared origin of these two malignancies has been further supported by numerous case reports describing a common isochromosome 12p in the corresponding tumor samples (Chaganti et al. 1989; Landanyi et al. 1990; Ikdahl et al. 2007). These studies laid the groundwork for a potential shared origin of the GCT and AML.

There are two distinct theories that have been generally postulated to explain how these two malignancies could arise from a shared founding clone. In the first, a primitive mesodermal stem cell is the founding clone and harbors the initiating alteration(s) that drives both cancers. The initiating cell would likely arise in early development in the aorta–gonad–mesonephros (AGM) region, which is the origin for stem cells that give rise to definitive hematopoiesis (Medvinsky and Dzierzak 1996). For unclear reasons, cells derived from the founding clone would remain in the AGM region but would also be present in the bone marrow—and could then give rise to both the GCT in the chest and the AML in the bone marrow. In the alternative theory, the AML is derived directly from cells from the GCT (mostly likely from the yolk sac component of a GCT). Some population of cells from the GCT "seed" (or metastasize to) the bone marrow, which gives rise to the AML (as reviewed in Zhao and Dowell 2012).

The argument for a shared common origin was strengthened by a recent study, which reported the results of targeted massively parallel sequencing of 33 genes, standard cytogenetic/fluorescence in situ hybridization analysis and single-nucleotide polymorphism (SNP) array profiling on samples from a patient with AML M7 and a synchronous mediastinal GCT. The authors identified shared somatic mutations in *PTEN* (G251V missense) and *TP53* (L130P missense), as well as the presence of isochromosome 12p, in both the GCT and AML samples, which further supports that a common founding clone initiated both cancers. However, both the *PTEN* and *TP53* mutations were present at relatively low variant allele frequencies (VAFs) in both samples in that study. For example, in the GCT, the *TP53* mutation was only present at a VAF of 5.97% and the *PTEN* mutation at a VAF of 15.12% (with VAFs of 20.35% and 27.59% in the AML sample, respectively) (Oshrine et al. 2014). The low VAFs were most likely due to low tumor cell content of the samples that were sequenced, and these data are most consistent with shared mutations present in the founding clone of both cancers.

Herein, we report the results of enhanced exome sequencing from a case of a male patient with a mediastinal GCT and synchronous AML M7. By sequencing minute amounts of tumor DNA, we were able to identify and validate shared somatic mutations in *TP53*, *PTEN*, and five other genes (of unknown pathogenic significance). Our data support the hypothesis that these shared alterations are present in the founding clone of the tumors. The copy-number analysis of the AML exome data revealed an amplification of Chromosome 12p (consistent with an isochromosome 12p), which was not detected on standard cytogenetics. We also identified a heterozygous germline variant in *FANCA* (S858R), which is known to be associated with Fanconi anemia but is of uncertain significance here. This is therefore the second case report to describe the presence of shared *TP53* and *PTEN* somatic mutations in the rare syndrome of concurrent GCT and AML M7, suggesting that these mutations synergize in an important way to contribute to these tumors.

RESULTS

Clinical Presentation

The patient was a 33-yr-old Caucasian male with no significant past medical history who presented with a 1-mo history of generalized weakness, a 40-pound weight loss, and dyspnea on exertion. His initial workup was notable for a platelet count of 5000/μL, hemoglobin of 13.1 g/dL, and a white blood count of 9200 cells/μL with a normal differential. A chest radiograph revealed evidence of a large anterior mediastinal mass; a computed tomography (CT) scan of the chest was performed that showed a 10 × 7.7 × 11-cm heterogeneous enhancing anterior mediastinal mass (Fig. 1). Given the suspicion for a GCT in this young man, standard tumor markers were drawn: α-fetoprotein (AFP) was 237 ng/mL (upper limit of normal [ULN] was 8.1 ng/mL), lactic acid dehydrogenase (LDH) was 6760 U/L (ULN 250 U/L), and β-human chorionic gonadotropin (β-hCG) was <5 (normal <5 IU/L). Given the patient's abnormal blood counts, a bone marrow biopsy was done and revealed a moderately fibrotic marrow with an abnormal population of large, mononuclear cells with irregular contours. The overall cellularity of the marrow was 70% from the core biopsy section (Fig. 2A). Immunostaining of the core showed that a subset of the large cells were $CD61^+$ and had weak CD117 expression. By cytochemistry, these cells were negative for myeloperoxidase and periodic acid-Schiff (PAS) staining with focal nonspecific esterase (NSE) positivity. Immunohistochemistry for GCT markers was negative (AFP, OCT4, placental alkaline phosphatase [PLAP], and SALL4). Overall, the CD61 immunostaining was consistent with megakaryoblasts (Fig. 2B). The hemodilute aspirate showed 15% large blasts with flow cytometry demonstrating that a subset of these blasts were $CD41^+$, $CD61^+$, and CD117dim ($CD34^-$ and $CD33^-$). Cytogenetic studies revealed a hyperdiploid karyotype: 59–69, XXY; +X, +2, −3, −4, −6, −8, +10, −11, −12, −13, −16, −18, +19, +20, +21, +1–4mar[composite karyotype in 9/25 metaphases]/46, XY[17]. Taken together, these findings were consistent with a diagnosis of acute megakaryoblastic leukemia, or AML M7 under the former French–American–British (FAB) classification (Bennett et al. 1976).

A CT-guided core needle biopsy of the mediastinal mass showed necrotic tissue with one island of viable cartilage cells suggestive of a GCT. The patient then underwent video-assisted thoracic surgery and incisional biopsy of the mediastinal mass, which revealed necrotic fragments of tissue with scattered foci of moderately to poorly differentiated

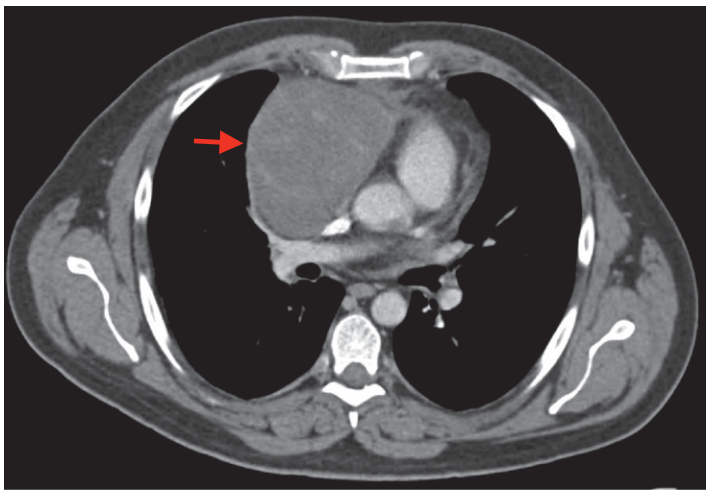

Figure 1. Computed tomography scan of the chest revealed a large, anterior mediastinal mass (red arrow).

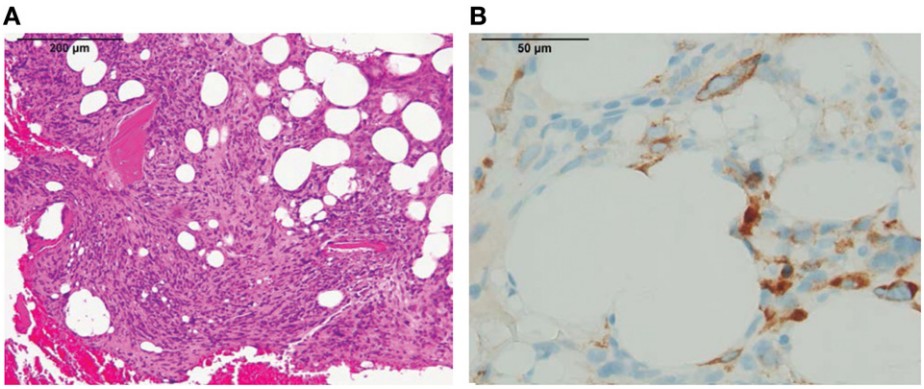

Figure 2. (*A*) A low-magnification (10×) view of a section from the diagnostic bone marrow biopsy shows a moderately fibrotic marrow, many infiltrating histiocytes, and an abnormal population of large, mononuclear cells. (*B*) A higher-magnification (40×) view of the diagnostic bone marrow section with immunohistochemistry highlighting the $CD61^+$ megakaryoblasts (brown staining).

adenocarcinoma (Fig. 3). Immunostaining was positive for pancytokeratin, CK7, and AFP reactivity, with nonreactivity for CK20, OCT4, SALL4, PLAP, TTF1, and napsin-A. Overall, the diagnosis was consistent with a nonseminomatous GCT. Other than the isolated island of cartilage from the first biopsy, we did not observe the presence of other germ layers. Specifically, there was no identified yolk sac component to either biopsy.

The initial pathologic diagnosis of both the AML M7 and GCT were difficult. The pathologic interpretation of the diagnostic bone marrow biopsy was complicated by marrow fibrosis and numerous background histiocytes (not uncommon in AML M7) and moderate crush artifact (Hahn et al. 2015). Although the case did not meet the World Health Organization (WHO) guidelines for a diagnosis of AML with >20% blasts, the aspirate with 15% blasts was hemodilute, and the overall findings were consistent with a diagnosis of AML M7

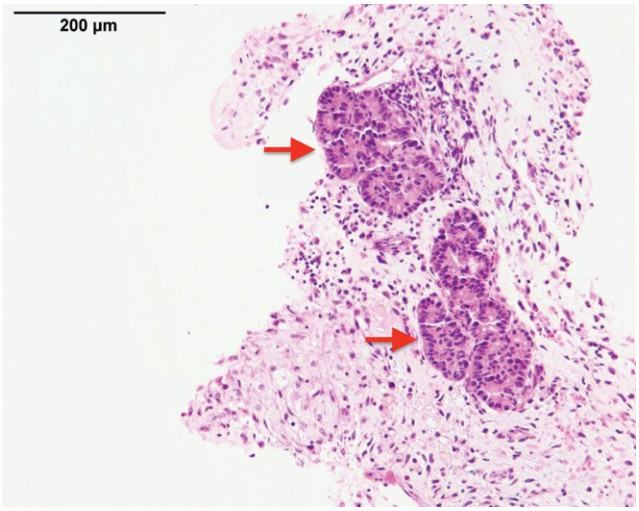

Figure 3. Low-magnification (10×) view of a section from the incisional biopsy of the mediastinal mass, which shows necrotic fragments of tissue with scattered foci of moderately to poorly differentiated adenocarcinoma (red arrows).

(Vardiman et al. 2002). Similarly, despite two biopsies, the diagnosis of the GCT was complicated by the extensive necrosis of the tumor samples. Nonetheless, it was clear that the disease in the bone marrow and the chest were two distinct malignancies. Furthermore, the issues with the suboptimal tumor samples led to unique challenges for comprehensive sequencing, which will be outlined in detail below.

The patient was initially treated with standard "7+3" AML induction chemotherapy (with cytarabine and idarubicin), and a day-15 bone marrow biopsy showed a hypocellular marrow with no evidence of leukemia. He then had a day-30 bone marrow biopsy, which showed a normocellular marrow with no evidence of leukemia. As his blood counts had recovered, he met the criteria for complete remission and went on to receive one cycle of high-dose cytarabine consolidation therapy for AML; however, shortly thereafter his GCT markers began to rise (AFP 683.8 ng/mL, LDH 346 U/L, and β-hCG 18 IU/L). He was then treated with two cycles of etoposide, ifosfamide, and cisplatin (VIP regimen) for his GCT. The patient did have improvement in his tumor markers with VIP, but further restaging with imaging was not yet performed.

Fifteen days after his second cycle of VIP, he presented with nausea, vomiting, and altered mental status. A brain magnetic resonance imaging (MRI) showed evidence of marked leptomeningeal enhancement, and a lumbar puncture with cerebrospinal fluid (CSF) cytology confirmed central nervous system relapse of AML M7. The patient was treated with seven doses of intrathecal cytarabine, and his CSF cytology cleared of blasts. Unfortunately, the patient's mental status deteriorated several weeks after the completion of his intrathecal chemotherapy, and he expired 5 mo after his initial diagnosis. Although an autopsy was not performed, the cause of death was presumed to be secondary to persistent central nervous system (CNS) involvement with leukemia.

Genomic Analysis

To study the possible clonal relationship between the GCT and AML, we assayed these tumor specimens using "enhanced exome sequencing," which augments a standard exome-capture reagent with additional probes covering the coding sequences for all 264 recurrently mutated genes (RMGs) that have been identified in AML (Cancer Genome Atlas Research Network 2013; see Methods). This approach typically provides ~100× median coverage over the standard exome-target regions but increases coverage of the RMG target space to an average of ~400×–500×. As noted above, the tumor samples were not optimal for sequencing studies. Therefore for the GCT, a pathologist performed laser capture microdissection on sections of the formalin-fixed paraffin-embedded (FFPE) block from the second mediastinal biopsy to isolate areas that appeared to have been viable tumor. We isolated a total of 2 ng of GCT genomic DNA (gDNA) via this method before exhausting the FFPE block. Next, as the cryopreserved cells from the diagnostic hemodilute bone marrow aspirate only contained 15% blasts, we performed flow cytometry–based cell sorting to enrich for the blasts using a gating strategy for viable $CD61^+$ leukemic blasts. We isolated a total of 48 ng of AML gDNA via this method. The low yields of gDNA necessitated using whole-genome amplification (WGA) on these samples to ensure that we could obtain sufficient DNA for exome-capture hybridization. We performed WGA on the entire GCT gDNA isolate (as described in the Methods) and on 8 ng of the AML gDNA prior to library generation, capture, and sequencing. The remaining 40 ng of AML gDNA was not amplified but used for library generation (with a unique barcode adaptor) and captured independently before sequencing. We isolated gDNA from a skin biopsy obtained at the time of the diagnostic bone marrow biopsy and sequenced as above as a "normal" comparator to define the somatic status of mutations.

A minimum of 20× coverage was achieved for 35%, 19%, 62%, and 98% of the exome-target space for the GCT WGA, AML WGA, AML gDNA, and the skin gDNA, respectively. The low sequence coverage obtained using WGA libraries was typical for amplified low-input DNA samples, as was the low coverage obtained from using only 40 ng of input gDNA for the unamplified AML capture (we typically use a minimum of 150 ng of input gDNA for an exome library).

The low coverage made variant calling challenging, so in addition to our standard variant calling pipeline, we used extensive manual review and Sanger validation of putative calls. For each of the three tumor libraries, there were thousands of putative variants called, but most were low-frequency artifacts, likely resulting from the WGA and/or insufficient coverage. By limiting the analysis to protein-coding regions and focusing on data from the sequencing of the higher-quality nonamplified gDNA from the AML, we filtered the list down to 47 variants that had VAFs of >15% in the AML gDNA sample and were putatively shared somatic events between the tumor samples. Manual review further culled this list to 29 potential variants, 10 of which we labeled "high confidence" (by manual review). We also included a *PTEN* mutation, despite it having low read support in the GCT sample, as it is a well-known tumor suppressor, and four other mutations that were not "high confidence" but did have supporting reads in all tumor samples (*ALG1LP9*, *RASAL3*, *MT-ND6*, and *CRTAC1*—none with established roles in cancer pathogenesis). In total, 15 mutations were chosen for Sanger validation. Out of the 15 candidate variants, seven variants were validated as somatic in both samples, two variants were validated as somatic in only the AML M7 sample, two variants were validated as germline mutations, one variant (a deletion) was not detected in any tumor library, and three were in amplicons that failed sequencing reactions. These three amplicon sequences matched multiple places on the targeted chromosomes, as it was not possible to design primers that were unique to the target. As a result, we likely generated a mixed polymerase chain reaction (PCR) product, which resulted in low-quality trace sequences (Table 1; Supplemental Fig. 1). Of the coding somatic variants that we validated, none has mutations at the identical amino acid position reported in COSMIC, other than *PTEN* and *TP53*, which do have recurrent mutations at each respective location (the mutation data were obtained from the Sanger Institute Catalogue Of Somatic Mutations In Cancer website, http://www.sanger.ac.uk/cosmic) (Bamford et al. 2004).

Of the seven somatic variants observed in both tumors, we detected a frameshift deletion in *TP53* (R213fs_del) and a missense mutation in *PTEN* (C136R) (Fig. 4). Both mutations had VAFs approaching 100% for both samples in the exome data suggesting that both mutations were homozygous (Fig. 4C). Consistent with this observation, our analysis of the gAML M7 data is consistent with loss of heterozygosity (LOH) for genomic segments including these two genes (Supplemental Table 1). Sequence coverage for the GCT samples was very low (with 14 and two reads, respectively), so the VAF estimates are less reliable for that sample. The Sanger trace for the *TP53* deletion appears homozygous in the GCT sample, but is not as clear for the *PTEN* mutation (Fig. 4A,B). To exclude an artifact as a consequence of WGA, we isolated 47 ng of total genomic DNA from the first mediastinal core biopsy of the GCT (predominantly necrotic tumor) and again performed Sanger sequencing for the *TP53* and *PTEN* alterations. The *PTEN* reaction failed; however, the *TP53* sequencing was successful and confirmed that the deletion appeared to be homozygous.

In addition to the shared somatic variant analysis, we performed copy-number analysis using the exome-sequence data from the gAML M7 sample and detected an amplification of Chromosome 12p consistent with an isochromosome 12 (Fig. 5). As noted in the Clinical Presentation subsection, the AML karyotype from conventional cytogenetics was extremely complex with evidence of -12 in the hyperdiploid [triploid] karyotype but no evidence of isochromosome 12p (there were several marker chromosomes that were not identified, however). We were unable to perform copy-number analysis on the exome data from the GCT

Table 1. Putative somatic variants with Sanger sequencing results

Chr	Reference genome sequence accession ID	GRCh37 position	Ref	Var	Type	HGVS DNA reference	Gene	Predicted effect	HGVS protein reference	Sanger	Skin ref	Skin var	Skin vaf	gAML ref	gAML var	gAML vaf	WGA AML ref	WGA AML var	WGA AML vaf	GCT ref	GCT var	GCT vaf
6	CM000668.1	37606083	A	C	SNP	g.37606083A>C	*MDGA1*	p.F896V	*p.Phe896Val*	AML	132	1	0.75	19	8	29.63	7	2	22.22	9	0	0
16	CM000678.1	4405237	G	A	SNP	g.4405237G>A	*CORO7*	p.T150I	*p.Thr150Ile*	AML	175	0	0	9	8	47.06	15	7	31.82	27	0	0
10	CM000672.1	89692922	T	C	SNP	g.89692922T>C	*PTEN*	p.C136R	*p.Cys136Arg*	AML +GCT	294	14	4.55	4	56	93.33	0	0	0	0	2	100
17	CM000679.1	7578213	A	-	DEL	g.7578213delA	*TP53*	p.R213fs	*p.Arg213fs*	AML +GCT	808	34	4.04	34	276	89.03	2	24	92.31	2	12	85.71
19	CM000681.1	15575174	G	C	SNP	g.15575174G>C	*RASAL3*	NULL	NULL	AML +GCT	62	2	2.63	10	11	45.83	31	20	28.57	33	14	24.56
MT	J01415.2	14372	C	A	SNP	g.14372C>A	*MT-ND6*	p.G101V	*p.Gly101Val*	AML +GCT	2127	51	2.29	10	336	97.11	0	5	100	10	34	77.27
2	CM000664.1	103324677	C	0	DEL	g.103324677delC	*SLC9A2*	p.Q725fs	*p.Gln725fs*	AML +GCT	196	4	2	7	8	53.33	46	25	35.21	13	10	43.48
3	CM000665.1	132068830	TCA	0	DEL	g.132068830_ 132068832delTCA	*ACPP*	p. I284in_frame _del	*p.Ile284del*	AML +GCT	157	1	0.63	23	14	37.84	3	2	40.00	53	45	45.92
11	CM000673.1	82880600	T	0	DEL	g.82880600delT	*PCF11*	p.F1075fs	*p.Phe1075fs*	AML +GCT	159	4	2.45	18	9	33.33	78	61	43.88	143	82	36.44
10	CM000672.1	99660359	C	G	SNP	g.99660359C>G	*CRTAC1*	e8+901	N/A	Fail	827	24	2.82	141	16	10.19	168	24	12.5	281	35	10.97
15	CM000677.1	84948847	T	C	SNP	g.84948847T>C	*RN7SL417P*	NULL	NULL	Fail	171	2	1.16	35	20	36.36	17	7	29.17	5	8	61.54
16	CM000678.1	15457598	G	A	SNP	g.15457598G>A	*NPIPA5*	p.A324V	*p.Ala324Val*	Fail	212	15	6.61	45	25	35.21	7	9	56.25	7	9	56.25
1	CM000663.1	12855648	A	G	SNP	g.12855648A>G	*PRAMEF1*	p.M310V	*p.Met310Val*	Germline	502	9	1.76	195	45	18.75	385	57	12.87	80	1	1.23
22	CM000684.1	23652503	T	C	SNP	g.23652503T>C	*BCR*	NULL	NULL	Germline	151	9	5.59	20	7	25.93	8	1	11.11	17	0	0
11	CM000673.1	71512862	G	–	DEL	g.71512862delG	*ALG1L9P*	NULL	NULL	WT	415	20	4.6	73	13	15.12	16	8	33.33	91	17	15.74

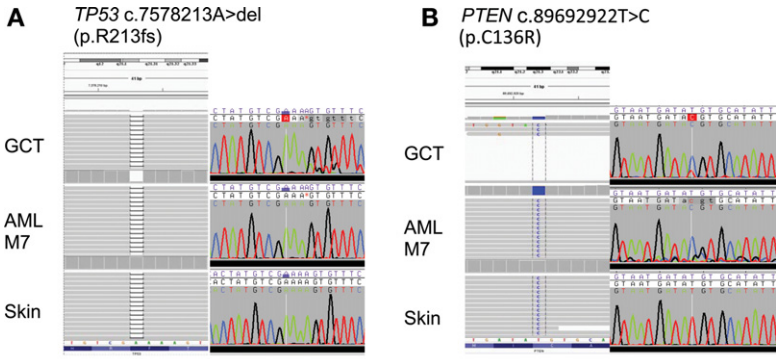

C

	TP53 (R213fs_del)	*PTEN* (C136R)
GCT	89%	100%
AML M7	85%	98%
Skin	4%	4%

Figure 4. Shared somatic mutations identified in *TP53* (*A*) and *PTEN* (*B*) using exome sequencing and later validated by Sanger sequencing. Variant allele fraction (VAF) of these two mutations is listed in *C*. Sanger sequencing for the *PTEN* and *TP53* variants was also done on unamplified gDNA isolated from the necrotic GCT (germ cell tumor) sample from the first mediastinal biopsy, which also confirmed the results depicted below. AML M7, acute megakaryoblastic leukemia.

because of the low coverage. Although amplification/isochromosome of 12p is the most common cytogenetic abnormality in GCTs, this feature is not common in AML (Nichols et al. 1985; Gibas et al. 1986; Bosl et al. 1989).

Finally, we performed a germline analysis on the high-quality exome data derived from the skin sample (see Supplemental Table 2). We detected a heterozygous germline variant in *FANCA* (S858R) that was validated by Sanger sequencing (at a VAF of 53% with 79 reference allele reads and 88 variant allele reads; see Supplemental Fig. 2 for Sanger validation results). This mutation is known to be associated with Fanconi anemia, an autosomal-recessive

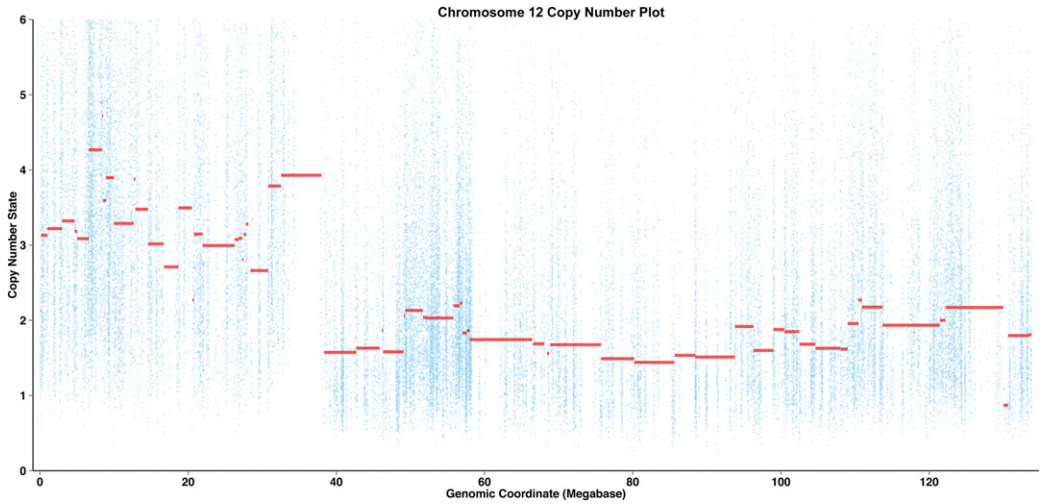

Figure 5. Copy-number analysis of the unamplified AML M7 sample demonstrated amplification of Chromosome 12p. The plot is "noisy" because of the low-sequencing coverage of the AML sample.

disorder (Savino et al. 2003). The mutation is of uncertain significance here as it is heterozygous, and no known complementation partner was identified.

DISCUSSION

The syndrome of associated hematologic malignancies and mediastinal GCTs is extremely rare but well documented in the literature (Nichols et al. 1985; Woodruff et al. 1995; Hartmann et al. 2000; Yu et al. 2011). A nonseminomatous mediastinal GCT and an associated hematologic neoplasm that most often involves the megakaryocytic lineage of hematopoiesis characterize the syndrome. This most commonly manifests as acute megakaryoblastic leukemia (AML M7); although, it has also been associated with myelomonocytic leukemia, myelodysplasia with abnormal megakaryocytes, and essential thrombocythemia (Nichols et al. 1985). Prior reports observed a median time of ~6 mo from the diagnosis of the GCT to diagnosis of the hematologic disease, with rare reports of a synchronous presentation, as seen in our patient (Nichols et al. 1985; Hartmann et al. 2000). Generally, this syndrome must be distinguished from a primary malignancy with a therapy-related secondary malignancy (i.e., a primary GCT and then a secondary AML, which typically develops at least a year following exposure to cytotoxic chemotherapy), but that potential scenario is not a complicating factor in this case (Nichols et al. 1985; Yu et al. 2011).

Isolated de novo AML M7 is also very rare in adults, only accounting for <1% of all AML cases. Outcomes for patients with isolated AML M7 are very poor, with a median overall survival reported between ~4 and 10 mo (Hahn et al. 2015). Similarly, a primary mediastinal nonseminomatous GCT is also a rare cancer, because extragonadal GCTs account for only <5% of GCTs in males. Primary mediastinal nonseminomatous GCTs (in the absence of an associated hematologic malignancy) also have a poor prognosis when compared with testicular (or extragonadal retroperitoneal) nonseminomatous GCTs with a 5-yr overall survival rate of only 45% (Bokemeyer et al. 2002).

The hematologic malignancies associated with primary mediastinal GCTs typically behave aggressively, with patients frequently succumbing to direct effects or complications of the hematologic malignancy, either before initiation of therapy or after achieving a short-lived response to treatment. The prognosis for these patients is extremely poor, with a median overall survival of only ~5 mo (Hartmann et al. 2000). Allogeneic stem cell transplant represents the only curative approach for patients, but few patients are able to move forward to transplantation (Hiramatsu et al. 2008).

Multiple theories have surfaced in an attempt to explain the connection between the GCT and AML. Previous reports have proposed that these malignancies originated from a common, early (i.e., mesodermal) stem cell progenitor, developing separately along germ cell and hematopoietic lines and resulting in the GCT and hematologic malignancy, respectively (Lee 1994). Alternatively, others have argued that the syndrome resulted from the differentiation of a transformed germ cell into the hematopoietic lineage (Bosl et al. 1989; Landanyi et al. 1990; Orazi et al. 1993). This proposed clonal relationship was initially established by the demonstration of isochromosome 12p in both GCT and hematologic malignancy specimens (Nichols et al. 1985; Hartmann et al. 2000; Yu et al. 2011). However, a later study presented evidence for hematopoietic cells within the yolk sac component of GCTs that morphologically resembled the leukemic blasts found in the bone marrow of four patients, suggesting that leukemia developed from a differentiated component of the GCT that subsequently "metastasized" to the bone marrow to cause leukemia (Orazi et al. 1993). Despite these findings, further elucidation of the genomic link between these malignancies has been slow to develop, on account of their rarity (Nichols et al. 1985, 1990; Chaganti et al. 1989; Woodruff et al. 1995; Yu et al. 2011). It should again be noted that

we did not identify a yolk sac component from the patient's GCT biopsies, which may have been a result of the extensive amount of necrosis present in these samples. This is one limitation of the current study in terms of defining the specific cell of origin of these two related tumors.

More recently, Oshrine et al. (2014) demonstrated shared mutations in *TP53* (L130P missense) and *PTEN* (G251V) in a male patient with concurrent AML M7 and a mediastinal nonseminomatous GCT. The patient also had evidence of isochromosome 12p in both cancers. In our case, enhanced exome sequencing was carried out on the AML M7 and GCT samples, and we identified common somatic mutations in *TP53* (R213fs_del) and *PTEN* (C136R missense), which were confirmed through Sanger sequencing. Importantly, we validated five additional shared mutations between the AML M7 and the GCT (in *RASAL3*, *MT-ND6*, *SLC9A2*, *ACPP*, and *PCF11*). Although the significance of any of these particular mutations to tumorigenesis is unknown (none are recurrently mutated in AML), the characterization of a total of seven shared somatic variants between the GCT and AML M7 firmly establishes the presence of a shared founding clone between the two distinct malignancies. Furthermore, as demonstrated in numerous previous reports, we were able to identify an amplification of Chromosome 12p in the AML M7, further supporting a common clonal ancestry. Unfortunately, we were not able to perform a copy-number analysis on the GCT given the data quality, and the limited coverage of the gAML precluded a detailed copy-number analysis, which is already difficult with exome data. An improved copy-number analysis of both the GCT and AML would have added power to our study and may have made it possible to infer the clonal evolution of the cancers. Moreover, as this was exome data, we also do not have information on structural variation, which should be recognized as another limitation of the current work.

We identified two variants that were specific to the AML M7 sample (in *MDGA1* and *CORO7*). Again, these variants have no clear link to AML leukemogenesis and are probably passenger mutations. It is also possible that they do not represent subclonal mutations that are specific to the AML sample—they may not have been detected in the GCT sample because of limitations associated with sequencing a WGA sample, including low sequence coverage and amplification-induced bias (Pinard et al. 2006). Other than the *TP53* mutation, we did not identify any other mutation in a gene that is known to be recurrently mutated in AML.

Germline analysis revealed a heterozygous germline variant in *FANCA* (S858R). The S858R mutation is known to be associated with Fanconi anemia, which is an autosomal-recessive disorder (Savino et al. 2003). The mutation is of uncertain significance in our patient, because it is heterozygous with no known complementation partner identified. It should be noted, however, that Oshrine et al. also found a heterozygous germline mutation of unknown significance, an *ATM* D1080E missense mutation, in their patient. Although involved in different pathways, both genes play pivotal roles in DNA damage repair.

PTEN mutations and isochromosome 12p are exceedingly rare in AML. We identified no *PTEN* mutations in the 200 cases of AML sequenced in the TCGA project (Cancer Genome Atlas Research Network 2013). Isochromosome 12p alterations are also as uncommon in AML, as previously shown in multiple studies (see Nichols et al. 1990). Conversely, *TP53* mutations are relatively rare in GCTs (Masters and Köberle 2003). We now report the second case to describe the association between shared *TP53* and *PTEN* mutations, as well as an alteration in Chromosome 12p, in the syndrome of concurrent GCT and AML M7. The mutual occurrence of a mutation in both *PTEN* and *TP53* has not been previously reported in AML, other than the current study and the study by Oshrine et al. (2014).

In summary, our data provide some of the strongest evidence to date that the tumors in this syndrome arise from a shared founding clone (i.e., a single cell ultimately evolved into both tumors). Given the limitations of our data, we could not deduce the clonal evolution

of the GCT and AML, however. More specifically, we could not determine whether the AML was a subclone of the GCT, which will require further study. Although speculative, mutations in both *TP53* and *PTEN*, along with isochromosome 12p, may represent the common genomic abnormalities that drive this rare syndrome that is distinct from the typical pathogenesis of either isolated AML or typical GCTs. Inactivation of *TP53* may partially explain the poor prognosis of these patients, because it is a known factor in chemoresistance and in unfavorable risk AML. Additional effort should be focused on the pathogenesis of this syndrome, because we have not been able to clarify the cell of origin. However, our results have significant implications for future genomic screening and on developing novel targeted treatment approaches for this rare patient population with an extremely poor prognosis.

METHODS

For the GCT, we extracted 2 ng of gDNA from laser capture microdissected tumor on the FFPE block of the incisional mediastinal biopsy. Briefly, tumor cells from hematoxylin and eosin–stained slides were identified by a pathologist (I.S.H.) and captured from 10-µm stained sections using an Arcturus PixCell instrument. The captured cells were then microdissected into the cap of 500-µL safe-lock tubes filled with 50 µL ALT buffer (QIAGEN). DNA extraction was performed as previously described (Cancer Genome Atlas Research Network 2013). WGA was performed using the Rubicon Genomics PicoPLEX WGA kit according to the manufacturer's instructions. We split the sample into three separate aliquots before amplification and then pooled these samples before sequencing to minimize the risk of bias introduced by the WGA. For the AML sample, 48 ng of gDNA was isolated from flow-sorted megakaryoblasts from cryopreserved cells banked during the diagnostic bone marrow biopsy. We performed flow sorting using a BD Bioscience FACSAria II cell sorter with a gating strategy for $CD61^+$ positive cells (CD45dim/low side scatter blasts that were $CD3^-$, $CD33^-$, and $CD61^+$). All antibodies were from BD Bioscience. For microscopy, we used an Olympus BX41 microscope with an Olympus DP72 camera.

Eight nanograms of the isolated AML gDNA was used for WGA libraries with the Rubicon Genomics PicoPLEX kit and the remaining 40 ng of unamplified gDNA was used for separate exome capture. For enhanced exome sequencing, we used the Roche NimbleGen SeqCap EZ Human Exome Library v3.0 kit plus a spike-in with probes covering all coding exons of significantly recurrently mutated genes in AML (from Integrated DNA Technologies, 264 genes, with the addition of the *TERT* promoter and *WT1* noncoding regions) (Cancer Genome Atlas Research Network 2013; Klco et al. 2015). The four dual-indexed libraries were then pooled and run on a single flow cell of an Illumina HiSeq 2500 sequencer in rapid run mode.

Sanger sequencing was done as previously described (Ellis et al. 2012) on the WGA AML and GCT DNA samples. In addition, we isolated 47 ng of gDNA (unamplified) from the core biopsy FFPE block of the first mediastinal GCT biopsy for Sanger sequencing for the *TP53* and *PTEN* mutations.

Exome-sequence data were aligned to reference sequence build GRCh37-lite-build37 using BWA-MEM version 0.7.7 (parameters: -t 4 -q 5::) (Li and Durbin 2009). Data were then merged and deduplicated using picard version 1.113 (https://broadinstitute.github.io/picard/). We detected somatic single-nucleotide variants (SNVs) using the union of three callers: (1) SAMtools version r982 (parameters: mpileup -BuDS) (Li et al. 2009) filtered by snp-filter version v1 and false-positive-filter v1 (parameters: –bam-readcount-version 0.4 –bam-readcount-min-base-quality 15 –max-mm-qualsum-diff 100) and intersected with Somatic Sniper version 1.0.4 (parameters: -F vcf -q 1 -Q 15) (Larson et al. 2012) filtered by false-positive version v1 (parameters: –bam-readcount-version 0.4 –bam-readcount-min-base-quality

Table 2. Exome-sequencing coverage metrics

Sample	Number of reads	Percentage of duplicate reads	Percentage of reads mapped	On target mean coverage
Skin	195,524,973	6.89	99.88	183.94
gDNA AML M7	50,171,683	6.07	99.88	38.11
WGA AML M7	44,068,667	4.1	99.3	17.66
WGA GCT	120,320,947	3.13	99.55	36.50

gDNA, genomic DNA; AML M7, acute megakaryoblastic leukemia; WGA, whole-genome amplification; GCT, germ cell tumor.

15) then somatic-score-mapping-quality version v1 (parameters: –min-mapping-quality 40 –min-somatic-score 40); (2) VarScan 2.3.6 (Koboldt et al. 2012) filtered by varscan-high-confidence version v1 then false-positive version v1 (parameters: –bam-readcount-version 0.4 –bam-readcount-min-base-quality 15); and (3) Strelka version 1.0.11 (parameters: isSkipDepthFilters = 1) (Saunders et al. 2012) (see Table 2 for coverage metrics).

We detected somatic indels using the union of four callers: (1) gatk-somatic-indel version 5336 (McKenna et al. 2010) filtered by false-indel version v1 (parameters: –bam-readcount-version 0.4 –bam-readcount-min-base-quality 15); (2) pindel version 0.5 (Ye et al. 2009) filtered by pindel-somatic-calls version v1 then pindel-vaf-filter version v1 (parameters: –variant-freq-cutoff=0.08) then pindel-read-support version v1; (3) VarScan 2.3.6 (parameters: –nobaq –version r982) (Koboldt et al. 2012) filtered by varscan-high-confidence-indel version v1; and (4) Strelka version 1.0.11 (parameters: isSkipDepthFilters = 1) (Saunders et al. 2012). Transcript annotation was performed using Ensembl v74_37. All somatic variants were manually reviewed using Integrative Genomics Viewer (IGV) (Robinson et al. 2011).

Somatic copy-number variants (CNVs) were called and recentered from the aligned BAM file using VarScan2 (http://dkoboldt.github.io/varscan) (Koboldt et al. 2012) using default parameters. Segments of copy number were identified using circular binary segmentation as implemented in DNAcopy for R (Seshan VE and Olshen A. DNAcopy: DNA copy-number data analysis R package, version 1.40.0). VarScan2 was also used in conjunction with the DNAcopy package to identify regions of copy-number-neutral LOH. For a list of all called CNVs from the gDNA AML sample, please see Supplemental Table 3.

Germline SNPs and indels were detected in the skin sample using SAMtools version r982 (parameters: -nobaq –version r982:–min-coverage 3 –min-var-freq 0.20 –p-value 0.10 –strand-filter 1 –map-quality 10) filtered by false-positive v1 (parameters –bam-readcount-min-base-quality: 15 –bam-readcount-version: 0.4 –max-mm-qualsum-diff: 100). These were unioned with SNPs called with SAMtools version r962 filtered by var-filter-snv v1, then false-positive-vcf v1 (parameters: –bam-readcount-min-base-quality: 15 –bam-readcount-version: 0.4 –max-mm-qualsum-diff: 100). Variants were filtered against an internally curated list of cancer-related genes, and then further curated to retain those likely to have functional consequences (Supplemental Table 2).

ADDITIONAL INFORMATION

Ethics Statement

The patient was enrolled in a single-institution, tissue-banking protocol approved by the human studies committee at Washington University. He provided written informed consent for comprehensive sequencing studies, including exome sequencing. The Washington University Institutional Review Board (IRB) approved this protocol.

Database Deposition and Access

The sequence data for all tumors and matched normal samples has been deposited in the NCBI database of Genotypes and Phenotypes (dbGaP; http://www.ncbi.nlm.nih.gov/gap) under accession number: phs000159.v8.p4. *PTEN* and *TP53* variants have been deposited in ClinVar (http://www.ncbi.nlm.nih.gov/clinvar/) under accession numbers SCV000257331–SCV000257340.

Acknowledgments

This work was done as part of the Washington University School of Medicine Genomics Tumor Board, which is a collaborative effort between the Division of Oncology and the McDonnell Genome Institute. The authors thank Drs. John F. Dipersio, Timothy J. Ley, Elaine R. Mardis, and Richard K. Wilson for their supervision, mentorship, and support of this project.

Author Contributions

C.L. analyzed data and wrote the manuscript. P.R. conceived parts of the study and wrote the manuscript. C.A.M. analyzed data and wrote the manuscript. I.S.H. performed experiments. P.W. conceived parts of the study. B.A.O. analyzed the data and wrote the manuscript. M.O., V.M., and R.T.D. performed experiments. E.J.D. performed experiments and wrote the manuscript. M.G., O.L.G, and L.D.W. conceived parts of the study, analyzed the data, and wrote the manuscript.

Competing Interest Statement

The authors have declared no competing interest.

Received August 28, 2015; accepted in revised form October 22, 2015.

Funding

The research was funded with private research support from the Division of Oncology and the McDonnell Genome Institute. L.D.W. is supported by the National Institutes of Health/National Cancer Institute (NIH/NCI) K08 CA166229. O.L.G. is supported by NIH/NCI K22 CA188163.

REFERENCES

Bamford S, Dawson E, Forbes S, Clements J, Pettett R, Dogan A, Flanagan A, Teague J, Futreal PA, Stratton MR, et al. 2004. The COSMIC (Catalogue of Somatic Mutations in Cancer) database and website. *Br J Cancer* **91:** 355–358.

Bennett JM, Catovsky D, Daniel MT, Flandrin G, Galton DA, Gralnick HR, Sultan C. 1976. Proposals for the classification of the acute leukaemias. French–American–British (FAB) co-operative group. *Br J Haematol* **33:** 451–458.

Bokemeyer C, Nichols CR, Droz J, Schmoll H, Horwich A, Gerl A, Fossa SD, Beyer J, Pont J, Kanz L, et al. 2002. Extragonadal germ cell tumors of the mediastinum and retroperitoneum: results from an international analysis. *J Clin Oncol* **20:** 1864–1873.

Bosl GJ, Dmitrovsky E, Reuter VE, Samaniego F, Rodriguez E, Geller NL, Chaganti RS. 1989. Isochromosomes of chromosome 12: clinically useful marker for male germ cell tumors. *J Natl Cancer Inst* **84:** 1874–1878.

Cancer Genome Atlas Research Network. 2013. Genomic and epigenomic landscapes of adult de novo acute myeloid leukemia. *N Engl J Med* **368:** 2059–2074.

Chaganti RS, Ladanyi M, Samaniego F, Offit K, Reuter VE, Jhanwar SC, Bosl GJ. 1989. Leukemic differentiation of a mediastinal germ cell tumor. *Genes Chromosomes Cancer* **1:** 83–87.

DeMent SH, Eggleston SC, Spivac JL. 1985. Association between mediastinal germ cell tumors and hematologic malignancies: report of two cases and review of the literature. *Am J Surg Pathol* **9:** 23–30.

Ellis MJ, Ding L, Shen D, Luo J, Suman V, Wallis J, Van Tine BA, Hoog J, Goiffon R, Goldstein TC, et al. 2012. Whole genome analysis informs breast cancer response to aromatase inhibition. *Nature* **486:** 353–360.

Gibas Z, Prout GR, Pontes JE, Sandberg AA. 1986. Chromosome changes in germ cell tumors of the testis. *Cancer Genet Cytogenet* **19:** 245–252.

Hahn AW, Li B, Prouet P, Giri S, Pathak R, Martin MG. 2015. Acute megakaryocytic leukemia: what have we learned. *Blood Rev* doi: 10.1016/j.blre.2015.07.005.

Hartmann JT, Nichols CR, Droz JP, Horwich A, Gerl A, Fossa SD, Beyer J, Pont J, Fizazi K, Einhorn L, et al. 2000. Hematologic disorders associated with primary mediastinal nonseminomatous germ cell tumors. *J Natl Cancer Inst* **92:** 54–61.

Hiramatsu H, Morishima T, Nakanishi H, Mizushima Y, Miyazaki M, Matsubara H, Kobayashi M, Nakahata T, Adachi S. 2008. Successful treatment of a patient with Klinefelter's syndrome complicated by mediastinal germ cell tumor and AML(M7). *Bone Marrow Transplant* **41:** 907–908.

Ikdahl T, Josefsen D, Jakobsen E, Delabie J, Fossa SD. 2007. Concurrent mediastinal germ-cell tumour and haematological malignancy: case report and short review of literature. *Acta Oncol* **47:** 466–469.

Klco JM, Miller CA, Griffith M, Petti A, Spencer DH, Ketkar-Kulkarni S, Wartman LD, Christopher M, Lamprecht TL, Helton NM, et al. 2015. Association between mutation clearance after induction therapy and outcomes in acute myeloid leukemia. *JAMA* **314:** 811–822.

Koboldt DC, Zhang Q, Larson DE, Shen D, McLellan MD, Lin L, Miller CA, Mardis ER, Ding L, Wilson RK. 2012. VarScan 2: somatic mutation and copy number alteration discovery in cancer by exome sequencing. *Genome Res* **22:** 568–576.

Landanyi M, Samaniego F, Reuter VE, Motzer RJ, Jhanwar SC, Bosl GJ, Chaganti RS. 1990. Cytogenetic and immunohistochemical evidence for the germ cell origin of a subset of acute leukemias associated with mediastinal germ cell tumors. *J Natl Cancer Inst* **82:** 221–227.

Larson DE, Harris CC, Chen K, Koboldt DC, Abbott TE, Dooling DJ, Ley TJ, Mardis ER, Wilson RK, Ding L. 2012. SomaticSniper: identification of somatic point mutations in whole genome sequencing data. *Bioinformatics* **28:** 311–317.

Lee KC. 1994. Hematopoietic precursor cells within the yolk sac tumor component are the source of secondary hematopoietic malignancies in patients with mediastinal germ cell tumors. *Cancer* **73:** 1535.

Li H, Durbin R. 2009. Fast and accurate short read alignment with Burrows–Wheeler transform. *Bioinformatics* **25:** 1754–1760.

Li H, Handsaker B, Wysoker A, Fennell T, Ruan J, Homer N, Marth G, Abecasis G, Durbin R; 1000 Genome Project Data Processing Subgroup. 2009. The sequence alignment/map format and SAMtools. *Bioinformatics* **25:** 2078–2079.

Masters JR, Köberle B. 2003. Curing metastatic cancer: lessons from testicular germ-cell tumours. *Nat Rev Cancer* **3:** 517–525.

McKenna A, Hanna M, Banks E, Sivachenko A, Cibulskis K, Kernytsky A, Garimella K, Altshuler D, Gabriel S, Daly M, et al. 2010. The genome analysis toolkit: a MapReduce framework for analyzing next-generation DNA sequencing data. *Genome Res* **20:** 1297–1303.

Medvinsky A, Dzierzak E. 1996. Definitive hematopoiesis is autonomously initiated by the AGM region. *Cell* **86:** 897–906.

Nichols CR, Hoffman R, Einhorn LH, Williams SD, Wheeler LA, Garnick MB. 1985. Hematologic malignancies associated with primary mediastinal germ-cell tumors. *Ann Intern Med* **102:** 603–609.

Nichols CR, Roth BJ, Heerema N, Griep J, Tricot G. 1990. Hematologic neoplasia associated with primary mediastinal germ-cell tumors. *N Engl J Med* **322:** 1425–1429.

Orazi A, Neiman RS, Ulbright TM, Heerema NA, John K, Nichols CR. 1993. Hematopoietic precursor cells within the yolk sac tumor component are the source of secondary hematopoietic malignancies in patients with mediastinal germ cell tumors. *Cancer* **71:** 3873–3881.

Oshrine BR, Olsen MN, Heneghan M, Wertheim G, Daber R, Wilmoth DM, Biegel JA, Pawel B, Aplenc R, King RL. 2014. Acquired isochromosome 12p, somatic *TP53* and *PTEN* mutations, and a germline *ATM* variant in an adolescent male with concurrent acute megakaryoblastic leukemia and mediastinal germ cell tumor. *Cancer Genet* **207:** 153–159.

Pinard R, de Winter A, Sarkis GJ, Gerstein MB, Tartaro KR, Plant RN, Egholm M, Rothberg JM, Leamon JH. 2006. Assessment of whole genome amplification-induced bias through high-throughput, massively parallel whole genome sequencing. *BMC Genomics* **7:** 216.

Robinson JT, Thorvaldsdóttir H, Winckler W, Guttman M, Lander ES, Getz G, Mesirov JP. 2011. Integrative genomics viewer. *Nat Biotechnol* **29:** 24–26.

Saunders CT, Wong W, Swamy S, Becq J, Murray LJ, Cheetham RK. 2012. Strelka: accurate somatic small-variant calling from sequenced tumor-normal sample pairs. *Bioinformatics* **28:** 1811–1817.

Savino M, Borriello A, D'Apolito M, Ciscuolo M, Del Vecchio M, Bianco AM, Di Perna M, Calzone R, Nobili B, Zatterale A, et al. 2003. Spectrum of FANCA mutations in Italian Fanconi anemia patients: identification of six novel alleles and phenotypic characterization of the S858R variant. *Hum Mutat* **4:** 338–339.

Vardiman JW, Harris NL, Brunning RD. 2002. The World Health Organization (WHO) classification of the myleooid neoplasms. *Blood* **100:** 2292–2302.

Woodruff K, Wang N, May W, Adrone E, Denny C, Feig SA. 1995. The clonal nature of mediastinal germ cell tumors and acute myelogenous leukemia. *Cancer Genet Cytogenet* **79:** 25–31.

Ye K, Schulz MH, Long Q, Apweiler R, Ning Z. 2009. Pindel: a pattern growth approach to detect break-points of large deletions and medium sized insertions from paired-end short reads. *Bioinformatics* **25:** 2865–2871.

Yu N, Kim HR, Cha YJ, Park EK, Kim JW. 2011. Development of acute megakaryoblastic leukemia with isochromosome (12p) after a primary mediastinal germ cell tumor in Korea. *J Korean Med Sci* **26:** 1099–1102.

Zhao GQ, Dowell JE. 2012. Hematologic malignancies associated with germ cell tumors. *Expert Rev Hematol* **5:** 427–437.